Variation in efficiency of DNA mismatch repair at different sites in the yeast genome

Joshua D. Hawk*, Lela Stefanovic*, Jayne C. Boyer*, Thomas D. Petes†‡§¶, and Rosann A. Farber*‡§‖**

*Department of Pathology and Laboratory Medicine, †Department of Biology, ‡Lineberger Comprehensive Cancer Center, §Curriculum in Genetics and Molecular Biology, and ‖Department of Genetics, University of North Carolina, Chapel Hill, NC 27599

Contributed by Thomas D. Petes, April 25, 2005

Evolutionary studies have suggested that mutation rates vary significantly at different positions in the eukaryotic genome. The mechanism that is responsible for this context-dependence of mutation rates is not understood. We demonstrate experimentally that frameshift mutation rates in yeast microsatellites depend on the genomic context and that this variation primarily reflects the context-dependence of the efficiency of DNA mismatch repair. We measured the stability of a 16.5-repeat polyGT tract by using a reporter gene (*URA3-GT*) in which the microsatellite was inserted in-frame into the yeast *URA3* gene. We constructed 10 isogenic yeast strains with the reporter gene at different locations in the genome. Rates of frameshift mutations that abolished the correct reading frame of this gene were determined by fluctuation analysis. A 16-fold difference was found among these strains. We made mismatch-repair-deficient (*msh2*) derivatives of six of the strains. Mutation rates were elevated for all of these strains, but the differences in rates among the strains were substantially reduced. The simplest interpretation of this result is that the efficiency of DNA mismatch repair varies in different regions of the genome, perhaps reflecting some aspect of chromosome structure.

genetic instability | microsatellite | mutation rate | *Saccharomyces cerevisiae*

Comparisons of amino acid or base sequences of orthologous genes indicate that different genes evolve at different rates (1). Differences in the rates of accumulation of amino acid changes or nonsynonymous base substitutions are influenced by selective constraints (1). For highly expressed genes, the rate of synonymous base substitutions is affected by GC content and codon bias (2, 3). In *Saccharomyces cerevisiae* and mammalian cells, the rates of synonymous substitutions also vary by a factor of ≈10, depending on the position of the gene in the genome (4–6). The interpretation of these observations is unclear. It is possible that the misincorporation rates of the replicative DNA polymerases are different at different positions in the genome. Alternatively, the fidelity of DNA polymerases may be invariant, but the detection and repair of misincorporation events may be context-specific.

Microsatellites are regions of DNA in which a single base or a small number of bases is repeated in tandem. The polyGT sequence is a particularly common microsatellite in many eukaryotes (7). We have developed (8, 9) methods of measuring the rate of microsatellite alterations. In this study, we used this assay to measure the mutation rates of the same polyGT microsatellite placed in 10 different chromosomal contexts in the yeast genome. We show that the microsatellite mutation rates vary by more than an order of magnitude among different genomic positions in yeast strains that have wild-type DNA mismatch repair. We have demonstrated (8) that the mutation rates of microsatellites are greatly elevated in yeast strains with deficient mismatch repair. In this study, we find that microsatellite instability is substantially elevated in all contexts examined; however, the relative differences between sites are reduced. This result demonstrates that different genomic regions have different efficiencies of DNA mismatch repair.

Materials and Methods

Strain Constructions. All strains were derived from the haploid MS71 (*α ade5-1 his7-2 trp1-289 ura3-52*) by transformation. LS48, which contains a complete deletion of the *ura3-52* allele, was generated by transforming MS71 with a PCR fragment resulting from amplifying the plasmid pA632 (containing a gene conferring resistance to hygromycin) (10), with the following primers: *URA3-F*, 5′-TCTTAACCCAACTGCACAGAACAAAAACCTGCAGGAAACGAAGATAAATCCGTAGCGTGCAGGTCGAC-3′; and *URA3-R*, 5′-GCTCTAATTTGTGAGTTTAGTATACATGCATTTACTTATAATACAGTTTTATCGATGAATTCGAGCTCG-3′. In the hygromycin-resistant transformants, the *HYG* gene replaces the *URA3* sequence. The strains with insertions of the *URA3-GT* reporter (which confers wild-type *URA3* activity) were constructed by transforming LS48 with PCR fragments generated by amplification of sequences derived from plasmid pMBW1 (see Fig. 1), which contains the *URA3-GT* fusion gene (9). Each primer was ≈75 bases in length, with the 5′ 45–55 bases representing yeast genome sequences flanking the insertion (Stanford University Saccharomyces Genome Database, http://genome-www.stanford.edu) and the 3′ bases representing sequences of pMBW1 flanking the *URA3-GT* fusion gene. The sequence at the 3′ end of the primers was either 5′-CTCGAGCGCTGATTAAATTACCCCAG-3′ (located upstream of the fusion gene) or 5′-GGATCCAATAACTGATATAAT-3′ (located downstream). The positions of the insertions in the genome were as follows: 74,422–74,423 on III (*ARS306-I*::*URA3-GT* and *ARS306-O*::*URA3-GT*), 210,606–210,696 on VI (*sup6*Δ::*URA3-GT*), 57,148–57,149 on III (*SRO9*::*URA3-GT*), 114,597–114,598 on III (*CEN3*::*URA3-GT*), 152,212–152,213 on V (*CEN5*::*URA3-GT*), 151,045–151,046 on XII (*CEN12*::*URA3-GT*), 946,305–946,395 on IV (*sup2*Δ::*URA3-GT*), 4,850–4,851 on III (*YCLWomega2*::*URA3-GT*), and 1,170–1,171 on III (*ARS300*::*URA3-GT*). The LS48 strain was transformed with the resulting fragments, selecting for Ura$^+$ transformants in galactose-containing medium, and the positions of the insertions were confirmed by PCR. We confirmed that the lengths of the microsatellite sequences in each strain were identical by measuring the sizes of PCR fragments using capillary electrophoresis with an Applied Biosystems Genetic Analyzer. Strains with a null allele of *msh2* (*msh2*::*kanMX*) were constructed by transformation using the described PCR primers and plasmid substrate (11).

Determination of Microsatellite Mutation Rates. For the assay of microsatellite instability, each strain with the *URA3-GT* reporter gene was grown on solid rich growth medium with 2% galactose (9). Dilutions of 20–50 individual colonies were plated on SG

Abbreviations: 5-FOA, 5-fluoroorotic acid; MMR, mismatch repair.

¶Present address: Department of Molecular Genetics and Microbiology, Duke University, Durham, NC 27710.

**To whom correspondence should be addressed at: Department of Pathology and Laboratory Medicine, University of North Carolina, CB 7525, Chapel Hill, NC 27599. E-mail: rfarber@med.unc.edu.

GENETICS

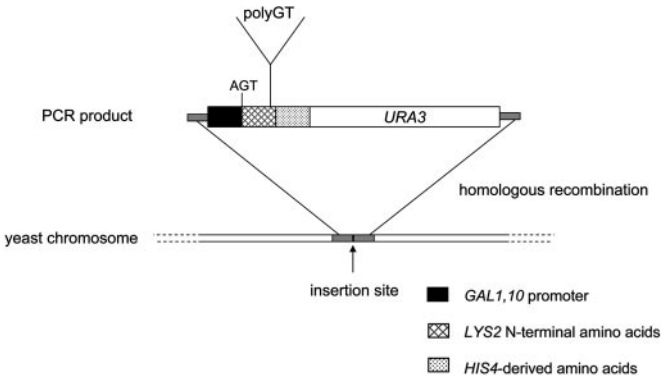

Fig. 1. Construction of yeast strains with the *URA3-GT* reporter gene in different chromosome contexts. The plasmid pMBW1 (9) contains a frameshift reporter gene (*URA3-GT*). This fusion gene has small segments derived from the yeast *LYS2* and *HIS4* genes, and most of the sequence of the yeast *URA3* gene. There is an in-frame insertion (33 bp) of polyGT sequences near the beginning of the gene, and transcription of the gene is controlled by the galactose-inducible *GAL1,10* promoter. The DNA fragments used for transformation were generated by PCR amplification of pMBW1 using primers that had homology to the sequences flanking the *URA3-GT* gene at their 3′ ends (≈20 bp) and homology to chromosomal DNA sequences at their 5′ ends. These fragments were transformed into the haploid yeast strain LS48 (deleted for *URA3*), and Ura$^+$ transformants were selected in galactose-containing medium.

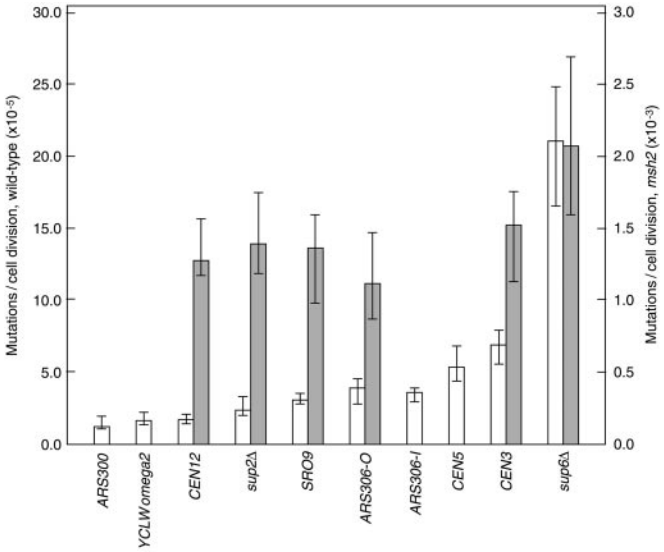

Fig. 2. Context-dependent rates of microsatellite instability in wild-type (MMR$^+$) and *msh2* mutant (MMR$^-$) yeast strains. White bars show the rates derived from MMR$^+$ cells, and gray bars show the rates for the isogenic MMR$^-$ strain; 6 of the 10 strains had an isogenic *msh2* derivative. (Absence of a gray bar indicates that an *msh2* derivative was not analyzed.) Error bars indicate the 95% confidence limits on the mutation rates.

(synthetic galactose) complete medium (to measure the number of cells per colony) or SG plus 5-fluoroorotic acid (5-FOA; to measure the frequency of Ura$^-$ derivatives). Rate estimates and 95% confidence limits for these estimates were calculated by using the method of the median, as described (9). Statistical tests of correlations between rates and other factors (such as GC content) were done by using the INSTAT program.

Measurement of Microsatellite Lengths. DNA was isolated from independent 5-FOA^R colonies, and PCR was performed by using primers with the following sequences that flank the microsatellite tract: 5′-CCAACGTGGTCATTTAATGAGC-3′ and 5′ HEX-GCTTGAACTCGTCTAATTTG-3′. The HEX tag (Synthegen, Houston) allows the PCR product to be detected by fluorescence. The sizes of the PCR fragments were measured by using capillary electrophoresis on the Applied Biosystems 310 Genetic Analyzer (for details, see ref. 12).

Results

We constructed 10 isogenic yeast strains with a *URA3-GT* reporter gene (see Fig. 1) including 16.5 in-frame GT-repeats (33 bp) at different locations in the genome. The locations of these constructs in the different strains were as follows: near the centromeres of three different chromosomes (*CEN3*::*URA3-GT*, *CEN5*::*URA3-GT*, and *CEN12*::*URA3-GT*), near a DNA replication origin *ARS306* (*ARS306-I*::*URA3-GT* and *ARS306-O*::*URA3-GT* at the same point of insertion but with opposite orientations of *URA3-GT*), near the telomere of chromosome III [*ARS300*::*URA3-GT* (1 kb from the telomere) and *YCLWomega2*::*URA3-GT* (5 kb from the telomere)], at the positions of tyrosine-tRNA genes (*sup2*Δ::*URA3-GT* and *sup6*Δ::*URA3-GT*), and near the middle of the left arm of chromosome III (*SRO9*::*URA3-GT*). All insertions were in intergenic regions, with the exception of the *SUP2* and *SUP6* insertions, in which the reporter gene replaced the coding sequence of the tRNA genes. The exact positions of the insertions are given in *Materials and Methods*.

Because the *URA3-GT* reporter has an in-frame microsatellite insertion, the strains were Ura$^+$; such strains are sensitive to 5-FOA. Thus, we could select derivatives of the starting strain that had an alteration in the microsatellite that resulted in loss of the correct reading frame (for example, an insertion or deletion of one repeat) by plating the cells on medium containing 5-FOA. For each of the 10 strains, we measured the frequency of 5-FOA-resistant derivatives in ≈20 independent cultures. These frequencies were converted to rates based on a fluctuation analysis. The rates ($\times 10^{-5}$ per division) and 95% confidence limits (shown in parentheses) for each mismatch repair (MMR)- proficient (MMR$^+$) strain were as follows: 1.3 (1–1.9), *ARS300*::*URA3-GT*; 1.7 (1.3–2.2), *YCLWomega2*::*URA3-GT*; 1.7 (1.4–2.0), *CEN12*::*URA3-GT*; 2.4 (2–3.3), *sup2*Δ::*URA3-GT*; 3.2 (2.8–3.5), *SRO9*::*URA3-GT*; 3.6 (2.9–3.9), *ARS306-I*::*URA3-GT*; 3.9 (2.8–4.5), *ARS306-O*::*URA3-GT*; 5.4 (4.4–6.7), *CEN5*::*URA3-GT*; 6.9 (5.6–7.8), *CEN3*::*URA3-GT*; and 21 (17–25), *sup6*Δ::*URA3-GT*.

A graphical summary of the rate measurements is shown in Fig. 2 (white bars). The rates varied between 1.3×10^{-5} per generation (*ARS300*::*URA3-GT)* to 21×10^{-5} per generation (*sup6*Δ::*URA3-GT*), a 16-fold difference. The two strains with telomeric insertions had the lowest rates of mutation, although these rates were not significantly different from the strains with the reporters at *CEN12* and *SUP2*. We chose to examine insertions at the *SUP2* and *SUP6* loci because Ito-Harashima *et al.* (5) had shown previously that the *SUP2* and *SUP6* tRNA genes mutated to become ochre suppressors at 20-fold-different frequencies, *SUP6* having the higher frequency. In our strains, in which *URA3-GT* replaced *SUP2* or *SUP6*, we found that the *sup6*Δ::*URA3-GT* strain had a 9-fold higher mutation rate than the *sup2*Δ::*URA3-GT* strain.

To determine the nature of the microsatellite alterations, we measured the sizes of the microsatellites in independent 5-FOA-resistant derivatives of each strain by PCR and capillary electrophoresis. As expected from previous studies in yeast (13), we found that most of the 5-FOA-resistant derivatives had a tract that was one repeat larger or smaller than the original 33-bp tract (Table 1). There was a ≈2-fold bias for insertions compared with deletions, as observed previously, although this bias was stronger for one of the strains (*CEN12*::*URA3-GT*). In approximately half of the 5-FOA-resistant derivatives of the strain with the

Table 1. Spectra of mutations observed in 5-FOA-resistant derivatives of the strains with the *URA3-GT* reporter gene (in bp)

Strain	−4	−2	0	+2	+4	Other
MMR$^+$						
ARS300::*URA3-GT*	0	4	1	5	0	0
YCLWomega2::*URA3-GT*	0	7	0	25	0	(−16)
CEN12::*URA3-GT*	0	1	1	36	1	(+16)
*sup2*Δ::*URA3-GT*	0	8	0	28	1	(−7, −7)
SRO9::*URA3-GT*	0	8	0	32	0	0
ARS306-I::*URA3-GT*	1	16	1	22	0	0
ARS306-O::*URA3-GT*	1	13	0	25	0	0
CEN5::*URA3-GT*	0	8	0	32	0	0
CEN3::*URA3-GT*	0	25	0	32	0	(−8, +14)
*sup6*Δ::*URA3-GT*	0	16	1	23	0	0
MMR$^-$						
CEN12::*URA-GT*	0	19	0	20	0	0
*sup2*Δ::*URA3-GT*	0	16	0	23	1	0
SRO9::*URA3-GT*	3	22	0	13	0	0
ARS306-O::*URA3-GT*	0	25	0	13	0	0
CEN3::*URA3-GT*	1	25	0	13	0	0
*sup6*Δ::*URA3-GT*	0	26	0	13	1	0

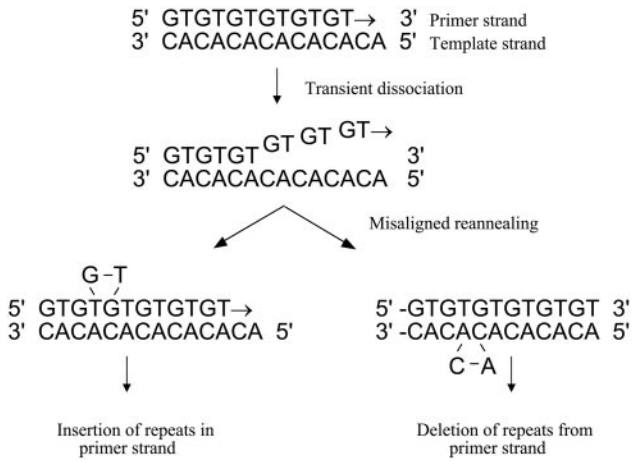

Fig. 3. Alterations in the length of a microsatellite by DNA polymerase slippage. Replication of a poly GT/CA tract that is seven repeats in length is shown. A slippage event in which the displaced repeat is on the primer strand, if uncorrected, will result in a tract that is eight repeats in length in the polyGT strand. Alternatively, a displaced repeat on the template strand results in six-repeat poly GT strand.

ARS300::*URA3-GT* insertion, the *URA3-GT* reporter gene was lost. This loss is probably the result of a gene conversion event between the reporter gene at *ARS300* with other subtelomeric regions, because the *ARS300* sequence is part of the subtelomeric X element that is represented at all of the yeast telomeres (14). This class of events was not included in the calculations of the microsatellite mutation rates shown in Fig. 2.

The Msh2 protein is required for DNA mismatch repair in yeast (15). Yeast strains that lack Msh2p have greatly increased rates of microsatellite mutations (8). We made *msh2* derivatives of six of the strains described above (*CEN12*::*URA3-GT*, *CEN3*::*URA3-GT*, *sup2*Δ::*URA3-GT*, *sup6*Δ::*URA3-GT*, *ARS306-O*::*URA3-GT*, and *SRO9*::*URA3-GT*). The rates of microsatellite alterations ($\times 10^{-3}$ per division) and 95% confidence limits for each MMR$^-$ strain were as follows: 1.3 (1.1–1.4), *CEN12*::*URA3-GT*; 1.4 (1.2–1.8), *sup2*Δ::*URA3-GT*; 1.4 (1–1.6), *SRO9*::*URA3-GT*; 1.1 (0.9–1.5), *ARS306-O*::*URA3-GT*; 1.5 (1–1.6), *CEN3*::*URA3-GT*; and 2.1 (1.6–2.7), *sup6*Δ::*URA3-GT*. These data are shown graphically as gray bars in Fig. 2. Although, as expected, the mutation rates for all of the microsatellites were substantially elevated in the MMR$^-$ strains, the differences among the mutation rates at different genomic sites were substantially reduced compared with the differences observed in the MMR$^+$ strains. [Note that the scales on the *y* axes for the MMR$^-$ (right axis) and MMR$^+$ (left axis) strains are different.] These results indicate that the context-dependence of mutation rates observed in wild-type strains reflects primarily the context-dependence of DNA mismatch repair rather than variation in the rates of replication errors.

We also examined the spectra of microsatellite alterations in the MMR$^-$ strains (Table 1). In contrast to the spectra observed in the MMR$^+$ strains, in which additions of a single repeat are more common than deletions of a single repeat, most of the MMR$^-$ strains had no bias or the opposite bias.

Discussion

These results provide direct experimental evidence for context-specific differences in the rates of frameshift mutations in microsatellite sequences. The loss or gain of repeats within microsatellites is likely to represent DNA polymerase slippage events (13). By this model (Fig. 3), during replication of a repetitive tract of DNA, the primer and template DNA strands temporarily dissociate and then reassociate out of alignment, leading to looping out of one or more repeats of the duplex (16). If the displaced repeat is on the primer strand, failure to correct this intermediate would result in an addition; if the displaced repeat is on the template strand, the resulting intermediate would result in a deletion.

In wild-type cells, it is thought that most of the resulting mismatches are corrected by the cellular DNA mismatch repair system. In support of this argument, cells that lack DNA mismatch repair have dramatically (>100-fold) elevated rates of microsatellite instability (8). As described above, for the 16.5 repeat polyGT tract in wild-type strains, additions are more common than deletions, whereas in the MMR$^-$ strains, approximately equal numbers of the two types of changes are observed. The simplest interpretation of this result, which has also been observed previously (13), is that DNA polymerase slippage results in equal numbers of mismatches in which the displaced repeats are located on the primer and template strands. The bias observed in the wild-type strain in favor of additions over deletions argues that the mismatches with a displaced repeat on the template strand are a better substrate for mismatch repair than those with a displaced repeat on the primer strand (13).

The context-dependence differences in microsatellite stability in wild-type strains could reflect context-dependence of the rate of polymerase slippage events, the efficiency of correction of mismatches by the cellular repair systems, or both factors. If the context-dependence of microsatellite stability primarily reflects context-dependence of mismatch correction, the differences among sites in mutation rates should be lost in cells with mutations that eliminate DNA mismatch repair. We find that the context-dependence of mutation rates is reduced from the 16-fold observed in wild-type strains to 2-fold. Thus, we conclude that much of the context-dependence of mutation rates reflects the relative efficiencies of DNA mismatch repair at the different sites. The comparison of mutation rates in the MMR$^-$ and MMR$^+$ strains allows calculation of the efficiency of repair at the various sites to be as follows: 99% (*CEN12*::*URA3-GT*), 98% (*sup2*Δ::*URA3-GT*), 98% (*SRO9*::*URA3-GT*), 96% (*ARS306-O*::*URA3-GT*), 95% (*CEN3*::*URA3-GT*), and 90% (*sup6*Δ::*URA3-GT*). However, it is likely that the efficiency of DNA mismatch repair is not the sole determinant of context-dependent effects on mutation rates, because the differences in

GENETICS

microsatellite stability for some strains (for example, *CEN12*::*URA3-GT* and *sup6*Δ::*URA3-GT*) are still statistically significant, even in the *msh2* background. Also, differences in mutation rates that are likely to be related to the site of insertion of the microsatellite have been observed in mismatch-repair-defective mammalian cells (17).

There is an alternative explanation for the observation that the context-dependence of microsatellite instability rates is higher in wild-type strains than in *msh2* strains. It is possible that some DNA polymerase slippage events occur at a time in the cell cycle (for example, outside of the S period) in which DNA mismatch repair is not active. This hypothesis would be consistent with our data if the frequency of this type of event is rare relative to DNA polymerase slippage events that occur during the S period (which are efficiently corrected in wild-type, but not *msh2*, strains) and the frequency of these events varies among different regions of the genome. This hypothesis requires the existence of a class of DNA polymerase slippage events that has not been reported.

DNA mismatch repair in eukaryotes is a complex process involving multiple steps (18–20). First, the mismatch is bound by a heterodimer of MutS homologues, either Msh2p/Msh6p (for base–base mismatches and one or two base loops) or Msh2p/Msh3p (for loops of 2–14 bp). This binding triggers an ATP-dependent conformational change that results in the recruitment of a MutL heterodimer (Mlh1p/Pms1p). The resulting ternary complex translocates along the DNA until a DNA nick [possibly bound by proliferating cell nuclear antigen (PCNA)] is encountered. The exonuclease Exo1p is recruited to the complex, resulting in excision of the nicked strand. This process (perhaps requiring multiple rounds of excision) eventually results in removal of the mismatch. The resulting single-stranded gap is filled in by DNA polymerase.

Although the efficiency of mismatch repair could be altered by affecting any of these steps described above, we suggest that the most likely steps to be affected are DNA mismatch recognition and DNA mismatch excision. For example, different regions of the chromosome may allow mismatch recognition to occur relatively efficiently or inefficiently. Marsischky and Kolodner (21) showed that the binding of the Msh2p–Msh6p complex to mismatches was affected by sequence context. Although these effects were local (≤18 bp from the mismatch), these studies do not preclude sequence context effects that can act at longer distances from the mismatch.

Alternatively, in different regions of the genome, the average distance between the mismatch and the nick that directs strand-specific removal could vary. Because the efficiency of mismatch repair is reduced as the distance between the mismatch and the nick is increased (21), this property could affect mutation rates. Pavlov *et al.* (22) showed that the efficiency of repair of an 8-oxoguanine-A mismatch was higher when the mismatch was on the lagging strand of the replication fork than when it was on the leading strand. This conclusion was based primarily on two observations. First, the reversion rate of a mutation (revertible by a C-to-A transversion) in an *ogg1* strain (deficient in the removal of 8-oxoguanine) depended on the orientation of the reporter gene with respect to the replication origin. Second, the rate differences observed for the two orientations were substantially reduced by mutations eliminating mismatch repair. The authors suggested that repair was more efficient on the lagging strand because the mismatches were closer to the nicks directing repair. Because we find that the orientation of the reporter relative to the replication origin does not have a significant effect on the rates of instability (comparison of the rates for *AR306-I*::*URA3-GT* and *ARS306-O*::*URA3-GT*), our results are not explained by this model unless additional conditions are operative. For example, it is possible that DNA polymerase slippage events occur more frequently on the lagging strand, which could balance the effect of more efficient DNA mismatch repair; however, even if this condition were met, it would not explain the variation in rates of instability of the reporter genes located at different genomic positions in our study.

Although we cannot determine which step of mismatch repair is affected by chromosomal context, we examined several chromosome properties including DNA replication, transcription, base composition, and chromatin structure. There does not appear to be a simple relationship between the efficiency of DNA mismatch repair and DNA replication. We compared the positions of the inserted reporter genes with the positions of active replication origins, as established by Raghuraman *et al.* (23). The four strains with insertions near active ARS elements (*ARS306-I*::*URA3-GT*, *ARS306-O*::*URA3-GT*, *CEN3*::*URA3-GT*, and *CEN12*::*URA3-GT*) had quite different rates of microsatellite instability; therefore, the position of the mismatch with respect to the replication origin does not appear to be important in determining the efficiency of the repair event. The expected times of replication (minutes from the beginning of the S period), based on the data of Raghuraman *et al.* (23) for the different insertions are as follows: 12 (*ARS306-I*::*URA3-GT* and *ARS306-O*::*URA3-GT*), 17 (*sup6*Δ::*URA3-GT*), 18 (*SRO9*::*URA3-GT*), 20 (*CEN3*::*URA3-GT* and *CEN5*::*URA3-GT*), 23 (*CEN12*::*URA3-GT*), 36 (*sup2*Δ::*URA3-GT*), 39 (*YCLWomega2*::*URA3-GT*), and 40 (*ARS300*::*URA3-GT*). We found no significant correlation between timing of replication and mutation rates ($P = 0.27$), although the two insertions with the lowest mutation rates were replicated latest in the S period.

In yeast, high rates of transcription result in elevated rates of mutation (9, 24). Because the *URA3-GT* reporter is expressed from the same strong promoter (*GAL1,10*) at all positions of the insertion, transcription is unlikely to be relevant to the effects observed in our experiments. Our results also suggest that similar context-dependent effects on mutations rates occur for both RNA polymerase III- and II-transcribed genes (tRNA genes and *URA3-GT*, respectively).

It has been argued that chromosomal regions of high G+C content may represent regions with relatively efficient DNA mismatch repair, because mismatch repair in yeast and mammals has a bias leading to increased G+C content (25, 26). Consequently, we looked for a correlation between mutation rates and the G+C content of the sequences in 1-, 5-, and 20-kb "windows" flanking the insertions. No significant correlations were found ($P > 0.4$ for all comparisons).

We suggest that the context-dependence of DNA mismatch repair efficiency is likely to reflect some aspect of chromatin structure that affects the recognition of the DNA mismatch, although other possibilities are not excluded. It is possible that MMR efficiency is a reflection of general chromatin "openness" (often associated with histone hyperacetylation and hypomethylation). Alternatively, the efficiency of repair could be affected by some particular pattern of histone modifications or the binding of nonhistone proteins. Given the plethora of such modifications and such proteins, it is likely to be a challenge to determine the mechanistic basis of these effects. Regardless of the details of the mechanisms, our results demonstrate that the DNA mismatch repair system operates with different efficiencies in different regions of the yeast genome, and that these differences influence mutation rates. These findings substantiate the hypothesis that differences in rates of evolution among genes result partly from variations in mutation rates in different genomic regions (4–6).

We thank Drs. T. Vision, R. M. Liskay, J. L. Argueso, K. Wolfe, P. Modrich, R. Kolodner, D. Gordenin, T. Kunkel, and S. Jinks-Robertson for useful discussions. This work was supported by National Institutes of Health Grants CA63264 (to R.A.F.) and GM24110 and GM52319 (to T.D.P.).

1. Nei, M. (1987) *Molecular Evolutionary Genetics* (Columbia Univ. Press, New York).
2. Sharp, P. A. & Li, W.-H. (1987) *Mol. Biol. Evol.* **4,** 222–230.
3. Ticher, A. & Graur, D. (1989) *J. Mol. Evol.* **28,** 289–298.
4. Wolfe, K. H., Sharp, P. A. & Li, W.-H. (1989) *Nature* **337,** 283–285.
5. Ito-Harashima, S., Hartzog, P. E., Sinha, H. & McCusker, J. H. (2002) *Genetics* **161,** 1395–1410.
6. Ellegren, H., Smith, N. G. C. & Webster, M. T. (2003) *Curr. Opin. Genet. Dev.* **13,** 562–568.
7. Tautz, D. & Renz, M. (1984) *Nucleic Acids Res.* **12,** 4127–4138.
8. Strand, M., Prolla, T. A., Liskay, R. M. & Petes, T. D. (1993) *Nature* **365,** 274–276.
9. Wierdl, M., Greene, C. N., Datta, A., Jinks-Robertson, S. & Petes, T. D. (1996) *Genetics* **143,** 713–721.
10. Goldstein, A. L. & McCusker, J. H. (1999) *Yeast* **15,** 1541–1553.
11. Kearney, H. M., Kirkpatrick, D. R., Gerton, J. L. & Petes, T. D. (2001) *Genetics* **158,** 1457–1476.
12. Hatch, S. B. & Farber, R. A. (2003) *Mut. Res.* **545,** 117–126.
13. Sia, E. A., Jinks-Robertson, S. & Petes, T. D. (1997) *Mut. Res.* **383,** 61–70.
14. Louis, E. J. (1995) *Yeast* **11,** 1553–1573.
15. Reenan, R. A. G. & Kolodner, R. D. (1992) *Genetics* **132,** 975–985.
16. Streisinger, G., Okada, Y., Emrich, J., Newton, J., Tsugita, A., Terzaghi, E. & Inouye, M. (1966) *Cold Spring Harbor Symp. Quant. Biol.* **31,** 77–84.
17. Hanford, M. G., Rushton, B. C., Gowen, L. C. & Farber, R. A. (1998) *Oncogene* **16,** 2389–2393.
18. Fishel, R. (1999) *Nat. Med.* **5,** 1239–1241.
19. Dzantiev, L., Constantin, N., Genschel, J., Iyer, R. R., Burgers, P. M. & Modrich, P. (2004) *Mol. Cell* **15,** 31–41.
20. Stojic, L., Brun, R. & Jiricny, J. (2004) *DNA Rep.* **3,** 1091–1101.
21. Marsischky, G. T. & Kolodner, R. (1999) *J. Biol. Chem.* **274,** 26668–26682.
22. Pavlov, Y. I., Mian, I. M. & Kunkel, T. A. (2003) *Curr. Biol.* **13,** 744–748.
23. Raghuraman, M. K., Winzeler, E. A., Collingwood, D., Hunt, S., Wodicka, L., Conway, A., Lockhart, D. J., Davis, R. W., Brewer, B. J. & Fangman, W. L. (2001) *Science* **294,** 115–121.
24. Datta, A. & Jinks-Robertson, S. (1995) *Science* **268,** 1616–1619.
25. Brown, T. C. & Jiricny, J. (1989) *Genome* **31,** 578–583.
26. Birdsell, J. A. (2002) *Mol. Biol. Evol.* **19,** 1181–1197.